CrossMark
click for updates

A regenerable copper mesh based oil/water separator with switchable underwater oleophobicity†

Yi Chen,[ab] Xinda Li,[a] Mary J. Glasper,[ac] Li Liu,[a] Hyun-Joong Chung*[a] and John A. Nychka*[a]

A Cu_2O coated Cu mesh with micro-scale surface structure was produced by a controlled UV-ozone treatment. The modified Cu mesh exhibited superhydrophilicity and underwater superoleophobicity. To achieve switchable wettability, the mesh's superhydrophilicity was converted to superhydrophobicity by application of a self-assembled monolayer (SAM) with stearic acid (SA), which can be repeatedly reversed to its original state (superhydrophilicity and underwater superoleophobicity) by UV treatment that causes SA decomposition. Gravity-driven kerosene/water separation was demonstrated with the separation efficiency remaining over 95% after 20 cycles for both "water-removal" and "oil-removal" separation modes.

Introduction

Dealing with oily wastewater and oil spills is an important environmental challenge around the world. Many scientists have investigated various techniques for separating oil/water mixtures by changing/altering material surface chemistry and roughness. There are three types of separation materials based on different separations: "oil-removing" materials, "water-removing" materials and smart separation materials.[1–3] "Oil-removing" materials are materials with superhydrophobicity and superoleophilicity.[4–8] For example, Zhu *et al.* developed *n*-dodecanethiol-coated superhydrophobic polyurethane (PU) sponges by taking inspiration from the adhesion of marine mussels;[4] Raza *et al.* created a polyacrylonitrile/polyethylene glycol nanofibrous membrane for oil/water separation.[5] However, these typical oil filtration or absorption membranes have shown that fouling and blocking issues can be caused by adhered oils. These adhered oils seriously affect the separation performance and decrease the membrane life time.

Recent research on materials with controlled surface structures that allow superhydrophilicity and underwater superoleophobicity opened a practically useful class of "water-removing" materials. Various superhydrophilic materials such as hydrogels, ZnO, $Cu(OH)_2$, graphene oxide, and cellulose have been utilized to construct underwater superoleophobic surfaces and create "water-removing" properties.[9–16] When the oil/water mixture is poured onto the membrane, the superhydrophilic surface will quickly absorb water and the whole interspace of the membrane will be occupied by water, which will prevent oil from passing through. The structure overcomes the oil fouling drawback of "oil-removing" type membranes, and results in high oil/water separation efficiency, durability and selectivity. Whereas switchable wettability (repeatable conversion from superhydrophilic/underwater superoleophobic to superhydrophobic/superoleophilic and *vice versa*) for oil/water separation is advantageous in terms of separating different concentration of oil/water mixtures (oil-rich or water-rich), slow conversion has limited its practical application. For instance, earlier studies required two weeks of storage time in dark atmosphere to switch surface wettability of ZnO coated mesh film from superhydrophilicity to superhydrophobicity.[17–19] Developing a simple, inexpensive, yet smart separation material with fast reversible surface wettability is imperative.[20]

Here, we report a new and fast switchable wettability Cu mesh for selective oil/water separation by combination with UV treatment and self-assembled monolayer (SAM) technique. Cu mesh is widely used for the oil/water separation due to its low cost, mechanical robustness and woven porous structure.[2,17,19,21–24] Firstly, superhydrophilic and underwater superoleophobic Cu_2O coated Cu mesh was obtained *via* UV-ozone oxidation of pristine Cu mesh while immersed in deionized water. In addition to the formation of Cu_2O, the underwater UV-ozone treatment also cleans the mesh surface by degrading adsorbed organic substances. Notably, the underwater UV exposure in 3D reflecting environment leads to effective UV exposure to entire inner surfaces of Cu mesh. The as-modified Cu mesh achieved oil/water separation by allowing water to

ᵃDepartment of Chemical and Material Engineering, University of Alberta, Edmonton, Alberta, T6G 1H9, Canada. E-mail: chung.hj13@ualberta.ca; jnychka@ualberta.ca

ᵇScion, Private Bag 3020, Rotorua, 3046, New Zealand

ᶜDepartment of Human Ecology, University of Alberta, Edmonton, Alberta, T6G 2N1, Canada

† Electronic supplementary information (ESI) available. See DOI: 10.1039/c6ra21099f

permeate through the mesh freely. Then, Cu_2O-coated mesh was immersed in a stearic acid (SA) solution, and the super-hydrophilicity was switched to superhydrophobicity after SA SAM modification. Subsequently, the wettability was switched back to its original state by UV treatment. This switchable wettability is also repeatable without apparent contact angle changes; the modified copper mesh offers a versatile strategy for rejuvenating oil/water separator by simple and inexpensive treatment.

Experimental

Preparation of Cu_2O coated Cu mesh

The original Cu mesh (McMaster-Carr, 100×100 wires per square inch; wire diameter $= 114$ μm) was cleaned with acetone and dried at 80 °C for 30 min. The cleaned mesh was then immersed in DI water, and UV treated in an UV-ozone chamber (Model No. 342, Jelight Company Inc., US; $\lambda < 243$ nm, with intensity of 22 mW cm^{-2}) at a distance 10 mm below the UV light source for a various time periods: 3 h, 5 h and 10 h. The walls of the water bath were covered with a 'rugged mirror' material that reflects UV light (for example, aluminum foil with substantial surface irregularity) to allow UV radiation from all directions. The as-treated mesh was then taken out and washed with DI water and ethanol.

Preparation of controllable surface wettability

The surface wettability was changed by alternating UV treatment and SA SAM coating.[17,20,21] Cu_2O coated mesh was first dipped into a 0.05 M stearic acid (SA)/ethanol solution for 1 h, followed by drying. To obtain opposite surface wettability, SA modified mesh was subsequently placed in the UV chamber for 1 h.

Characterization

Scanning electron microscopy (SEM) images were captured with a Vega-3 (Tescan, Czech Republic). Thin film X-ray diffraction (XRD) patterns were collected by X-ray diffractometry (Rigaku Ultima IV, Japan) with Cu-K radiation. The XRD data was collected over a 2θ range of 20° to 80°. The chemical bonding characteristics were analyzed *via* Fourier transform infrared (FTIR, Thermo Nicolet 8700) with attenuated total reflection (ATR) mode. Apparent contact angles of the surfaces were measured using a VCA Optima drop shape analyzer (AST Products Inc., USA) with 5 μL water or oil droplets. For underwater oil contact angle measurements, the modified Cu mesh was first placed into a transparent chamber with water. A 5 μL 1,2-dichloroethane (DCE, Sigma-Aldrich) was then dropped onto the mesh substrate and the apparent contact angle was measured.

Oil/water separation

Generally, due to the density difference between water and oils, it is hard to collect water or oil when the surface is hydrophobic. Lu *et al.* developed a "V" shaped mesh geometry (or basket vessel shape) for gravity-induced oil/water separation. The "V"

shape shifts the oil/water interface out of the plane of the filter and allows both oil and water to always be in contact with the mesh area and to drain either liquid through the mesh – thus resulting in a simple and fast oil/water separation and collection.[22] However, the "V" shape is very limited for practical application due to its small separation volume. Li *et al.* developed a funnel-like separation system (a rotated "V" cone), which has more contact surface.[23] The funnel-like system was employed herein for both superhydrophobicity and underwater superoleophobicity based oil/water separation. Here, we selected kerosene (purum, Sigma-Aldrich) as the model oil. The kerosene was dyed with Oil Red O (Sigma-Aldrich) for visualization.

Results and discussion

Fig. 1 shows the oxidation process of Cu mesh under UV-ozone treatment. Ozonation has been widely used in contaminated water treatment. In the presence of water, the decomposition of the aqueous ozone can generate hydroxyl radicals (OH) which are highly oxidizing agents:[24,25]

$$O_3 + H_2O \xrightarrow{h\nu(\lambda=254\ nm)} H_2O_2(aq) + O_2 \qquad (1)$$

$$H_2O_2 \xrightarrow{h\nu(\lambda=254\ nm)} 2OH \qquad (2)$$
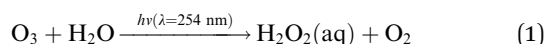
The Cu mesh was subsequently oxidized by highly reactive hydroxyl radical resulting in an oxide layer formed on the Cu surface, where Cu_2O was the major product. The oxidation reaction can be described as:[25]

$$2OH + 2Cu \rightarrow Cu_2O + H_2O \qquad (3)$$
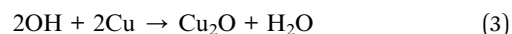
The transformation from Cu to Cu_2O is more preferable than Cu to CuO, due to the potential for oxidation of Cu to Cu_2O being much smaller than Cu to CuO.[26,27] This approach is done in the absence of chemicals such as strong alkaline or acid, indicating the potential for industrial-scale production.[28–30]

Fig. 2 shows the SEM images of the pristine and Cu_2O coated mesh at different UV-ozone treatment times. Fig. 2a is a low magnification SEM image of the Cu mesh with an average wire diameter of approximately 110 μm (100 mesh size) and smooth
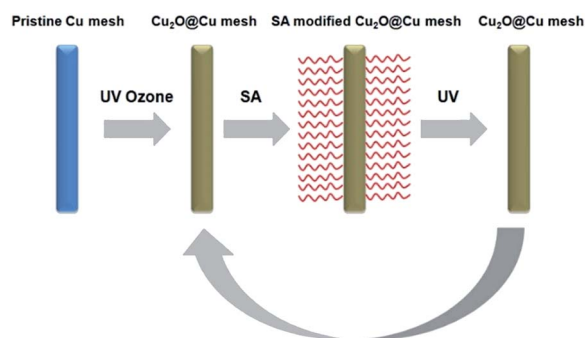

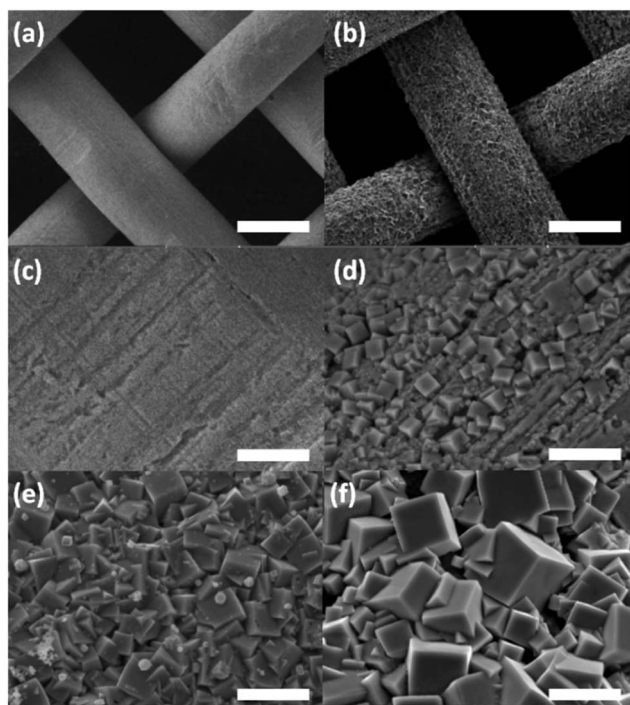**Fig. 1** Schematic illustration of the formation of switchable wettability Cu mesh.

Fig. 2 Low magnification SEM images of (a) control mesh 0 h, (b) 10 h UV-ozone treated Cu mesh with scale bar of 100 μm. High magnification SEM images of (c) control mesh 0 h; (d) 3 h; (e) 5 h and (f) 10 h UV-ozone treated Cu mesh; scale bar is 10 μm.

as manufactured surface. Fig. 2b shows the low magnification SEM image of mesh after 10 h UV-ozone treatment; micronsized cubic structures (Cu_2O crystals) are present on the surface. Fig. 2c–f indicates the corresponding high magnification SEM images of pristine, 3 h, 5 h, and 10 h UV-ozone treated mesh, respectively. Longer treating time leads to formation of larger cubic crystals of Cu_2O.

Fig. 3 presents the XRD patterns of the mesh before and after UV-ozone oxidative treatment. Both the pristine and as-modified mesh showed strong and sharp XRD peaks corresponding to the (111), (200), and (220) crystal planes of cubic
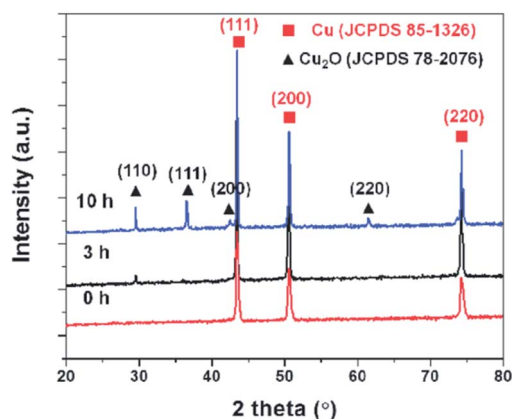
phase Cu (JCPDS no. 85-126). In addition, peaks attributed to the (110), (111), (200) and (220) crystal planes of cubic Cu_2O (JCPDS no. 78-2076) were detected after UV-ozone treatment.[25,31,32] No other peaks were observed in the XRD patterns. It is clear that the Cu oxidation after the UV-ozone treatment is cubic Cu_2O. The corresponding peaks became more intense and narrower with the increase of the UV-ozone treatment time indicating increasing crystal amounts and grain size growth.

The surface wettability of the as-coated mesh was characterized by apparent contact angle (CA) measurement. Fig. 4a displays that the water CA of $Cu_2O@Cu$ mesh is close to 0°, the water droplet quickly spread and permeated the mesh. In contrast, the underwater oil CA tended to 151°, additionally, according to the reformed macroscopic Cassie–Baxter model, the underwater oil apparent CA of treated copper mesh can be calculated as:[33,34]

$$\cos \theta^{CB} = \frac{D(\pi - \theta_e)\cos \theta_e}{D + d} + \frac{D \sin \theta_e}{D + d} - 1 \qquad (4)$$

where θ_e is the underwater oil equilibrium CA on a smooth surface (copper foil), D is the mesh wire diameter, and d is half opening width. The θ_e of copper foil treated for 10 h was measured to be ~120°. The predicted apparent contact angle of oil on copper mesh UV-ozone treated for 10 h in water is 142°. Compared with measured underwater oil CA of 10 h copper mesh (~151°, Fig. 4b), the predicted value was slightly smaller. Possibly, this difference was due to the fact that the surface area is further increased due to the roughness of the oxidized copper of the modified mesh (see Fig. 2), leading to a more pronounced Cassie effect. The result shows that the underwater hydrophobicity was further increased by introducing macroscopic woven structure, which is in favour of oil/water separation.

Next, CA of water on oxidized mesh with SAM modification was investigated. The SA modified mesh showed superhydrophobicity with a water CA of 157° (Fig. 4c) whereas the oil CA was close to 0° (Fig. 4d). The opposite wettability of SA modified mesh results in the capacity of "oil-removing" oil/water separation.
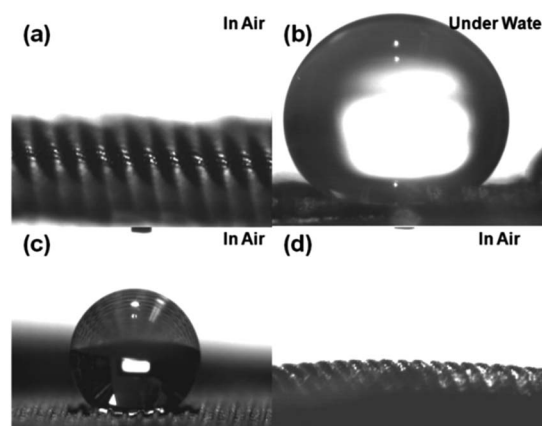

Fig. 3 XRD pattern of Cu mesh before and after ozone UV treatment (3 and 10 h). The ozone UV treatment produces Cu_2O.

Fig. 4 Optical images of apparent CAs on the copper mesh. (a) Water CA on Cu_2O coated mesh. (b) Oil CA on coated mesh. (c) Water CA on SA modified $Cu_2O@Cu$ mesh. (d) Oil CA on SA modified $Cu_2O@Cu$ mesh in air.

The gravity driven kerosene/water mixture (50% v/v) separation was performed by using the copper mesh as the separator. As shown in Fig. 5a–c, once the kerosene/water mixture was poured onto the pre-wetted Cu$_2$O@Cu mesh, the water quickly passed through the mesh to the conical beaker. The UV-visible absorption spectrum of collected water was compared with dyed kerosene and reference water (Fig. S1†). The absent of characteristic peak for Oil Red (518 nm) suggests that no visible oil (dyed) remains in the collected water. The separation efficiency was calculated according to $\eta = (m_1/m_0) \times 100\%$, where m_0 and m_1 are the mass of water before and after the separation, respectively.[8,22,35] The average efficiency of 20 separation cycles was 96.5% with no systematic decrease in separation efficiency (Fig. 5g).

After the mesh was rinsed with water, the Cu$_2$O coated mesh was immersed in a SA solution, followed by being dried and used for oil/water separation ("oil-removing"). As seen in Fig. 5d–f, the dyed oil (red) permeated freely through the superhydrophobic mesh due to the superhydrophobicity and superoleophilicity of SA modified mesh. Here, one may wonder how oil, which has a lower density than water can pass through copper mesh when water exists on top of the SA coated copper mesh. The 'conical shape' of the mesh is helpful in practice; the cone's volume needs to be bigger than the total volume of water so that oil's contact to the mesh is not blocked. The blocked water was collected and the oil content in the water was further determined by UV-visible absorption spectra (Fig. S1†). The result indicates that the blocked water absorption spectrum closely aligns with the reference water absorption spectrum, which prove that there was no oil left in the blocked water. The average separation efficiency of 20 separation cycles was around 97.6% (Fig. 5h).

The reversibility of wettability was studied by alternating UV treatments and SA SAM coating stages. Due to the UV-induced decomposition of the coated SA monolayer in the presence of a photocatalyst (Cu$_2$O), the superhydrophobic SA modified mesh could be easily switched to superhydrophilic mesh via UV irradiation treatment.[17,18,36,37] FTIR was used to indicate the presence of SA on the surface of modified mesh (Fig. 6a). The two peaks at 3000–2750 cm^{-1}, which represented CH$_3$ and CH$_2$ stretching were observed after SA modification,[9,37–39] and the intensity of these peaks clearly decreased after 1 h UV
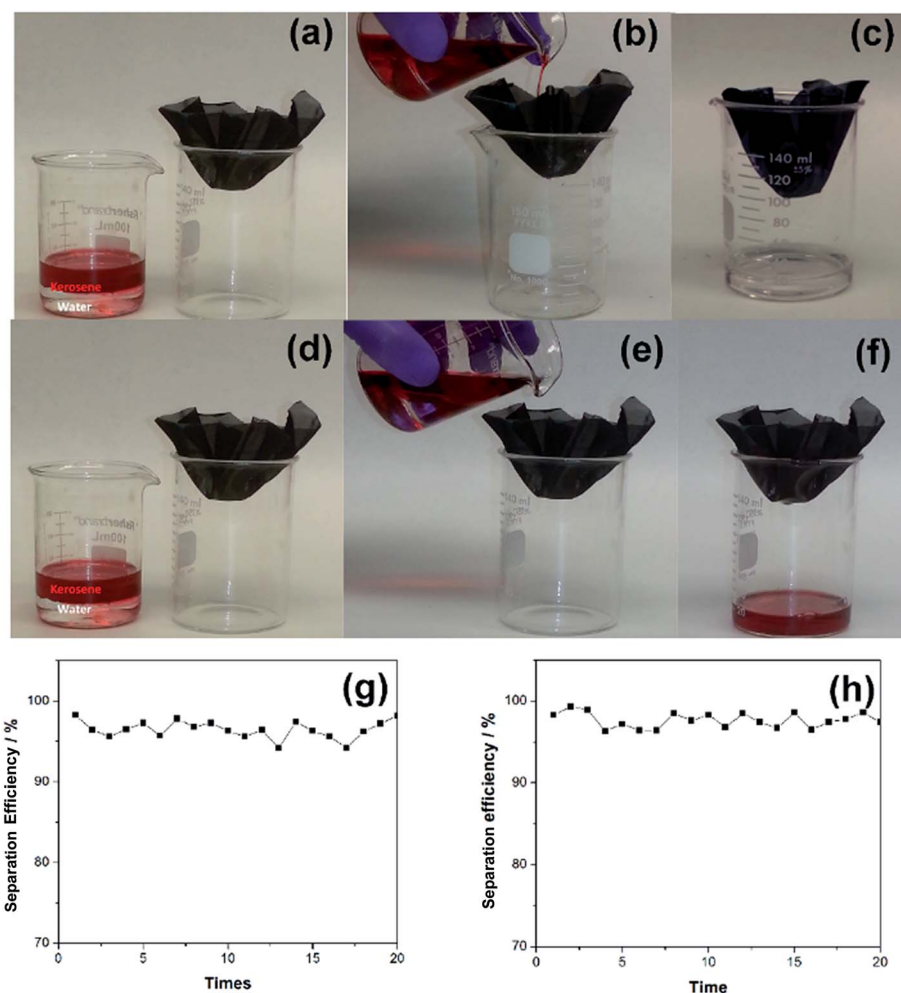

Fig. 5 Photograph of the controllable oil/water separation process. (a)–(c) Separation of water from oil by the Cu$_2$O@Cu mesh. The oil used here was kerosene dyed with Oil Red O for contrast. (d)–(f) Separation of oil from water by SA coated mesh. (g) Separation efficiency of the Cu$_2$O@Cu mesh by taking kerosene/water mixture as example. (h) Separation efficiency of SA modified mesh by taking kerosene/water mixture as example.
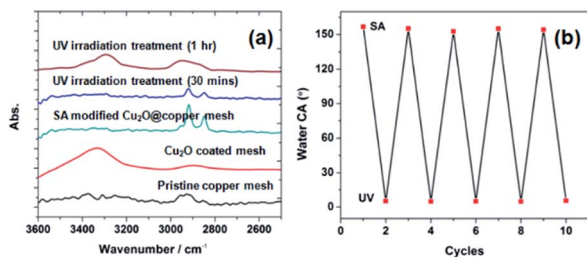
Fig. 6 (a) FTIR spectra of Cu mesh after treatments. (b) Reversibility of apparent water CA on the Cu_2O modified mesh by alternate SA immersion and UV treatment.

treatment. Subsequently, the superhydrophilicity was switched to superhydrophobicity again after SA modification. This process was repeated over 10 times and showed no obvious change of water CA, indicating good reversibility of wettability (Fig. 6b).

Conclusions

The commercial Cu mesh was successfully modified with Cu_2O *via* a facile and solution-based UV-ozone treatment method. The micro-structured Cu_2O@Cu mesh exhibited outstanding superhydrophilicity and underwater superoleophobicity, which effectively prevented the mesh surface from oil fouling in the conditions tested. The wettability of the as-modified mesh was easily reversed and regenerated by SAM technique and UV treatment. Kerosene/water separation was demonstrated to show high separation efficiency (>95%) and it also remained high after 20 cycles. The described approach was relatively facile, rapid, and yielded effective and efficient separation with switchable wettability, and provides new insights into the potential design of larger scale applications based on controllable surface wettability.

Acknowledgements

Notes and references

1 L. Wen, Y. Tian and L. Jiang, *Angew. Chem., Int. Ed.*, 2015, **54**, 3387.

2 B. Wang, W. Liang, Z. Guo and W. Liu, *Chem. Soc. Rev.*, 2015, **44**, 336.

3 Z. Xue, Y. Cao, N. Liu, L. Feng and L. Jiang, *J. Mater. Chem. A*, 2014, **2**, 2445.

4 Q. Zhu and Q. Pan, *ACS Nano*, 2014, **8**, 1402.

5 A. Raza, B. Ding, G. Zainab, M. EI-Newehy, S. S. AI-Deyab and J. Yu, *J. Mater. Chem. A*, 2014, **2**, 10137.

6 J. Li, L. Yan, H. Li, J. Li, F. Zha and Z. Lei, *RSC Adv.*, 2015, **5**, 53802.

7 J. Li, L. Yan, Y. Zhao, F. Zha, Q. Wang and Z. Lei, *Phys. Chem. Chem. Phys.*, 2015, **17**, 6451.

8 D. Ge, L. Yang, C. Wang, E. Lee, Y. Zhang and S. Yang, *Chem. Commun.*, 2015, **51**, 6149.

9 W. Zhang, Y. Cao, N. Liu, Y. Chen and L. Feng, *RSC Adv.*, 2014, **4**, 51404.

10 J. Li, D. Li, W. Li, H. Li, H. She and F. Zha, *Sep. Purif. Technol.*, 2016, **168**, 209.

11 Y. Chen, L. Liu, H. Chung and J. A. Nychka, *RSC Adv.*, 2015, **5**, 91001.

12 Z. Xue, S. Wang, L. Lin, L. Chen, M. Liu, L. Feng and L. Jiang, *Adv. Mater.*, 2011, **23**, 4270.

13 G. Wang, Y. He, H. Wang, L. Zhang, Q. Yu, S. Peng, X. Wu, T. Ren, Z. Zeng and Q. Xue, *Green Chem.*, 2015, **17**, 3093.

14 Y. Dong, J. Li, L. Shi, X. Wang, Z. Guo and Q. Liu, *Chem. Commun.*, 2014, **50**, 5586.

15 J. Li, H. M. Cheng, C. Y. Chan, P. F. Ng, L. Chen, B. Fei and J. H. Xin, *RSC Adv.*, 2015, **5**, 51537.

16 W. Zhang, Y. Zhu, X. Liu, D. Wang, J. Li, L. Jiang and J. Jin, *Angew. Chem.*, 2014, **53**, 856.

17 D. Tian, X. Zhang, Y. Tian, Y. Wu, X. Wang, J. Zhai and L. Jiang, *J. Mater. Chem.*, 2012, **22**, 19652.

18 H. Liu, L. Feng, J. Zhai, L. Jiang and D. Zhu, *Langmuir*, 2004, **20**, 5859.

19 D. Tian, Z. Guo, Y. Wang, W. Li, X. Zhang, J. Zhai and L. Jiang, *Adv. Funct. Mater.*, 2014, **24**, 536.

20 J. Li, D. Li, Y. Yang, J. Li, F. Zha and Z. Lei, *Green Chem.*, 2016, **18**, 541.

21 M. S. Lim, K. Feng, X. Chen, N. Wu, A. Raman, J. Nightingale, E. S. Gawalt, D. Korakakis, L. A. Hornak and A. T. Timerman, *Langmuir*, 2007, **23**, 2444.

22 Y. Lu, S. Sathasivam, J. Song, F. Chen, W. Xu, C. J. Carmalt and I. P. Parkin, *J. Mater. Chem. A*, 2014, **2**, 11628.

23 J. Li, R. Kang, X. Tang, H. She, Y. Yang and F. Zha, *Nanoscale*, 2016, **8**, 7638.

24 H. Lin and G. S. Frankel, *Corros. Eng., Sci. Technol.*, 2013, **48**, 461.

25 D. Liang, H. C. Allen, G. S. Frankel, Z. Y. Chen, R. G. Kelly, Y. Wu and B. E. Wyslouzil, *J. Electrochem. Soc.*, 2010, **157**, C146.

26 Y. Feng, K. S. Siow, W. T. Tao, K. L. Tan and A. K. Hsieh, *Corrosion*, 1997, **53**, 389.

27 A. Palit and S. O. Pehkonen, *Corros. Sci.*, 2000, **42**, 1801.

28 K. Chen, S. Song and D. Xue, *CrystEngComm*, 2013, **15**, 144.

29 Y. Qian, F. Ye, J. Xu and Z. Le, *Int. J. Electrochem. Sci.*, 2012, 7, 10063.

30 T. Notoya, *J. Mater. Sci. Lett.*, 1991, **10**, 389.

31 H. Pang, F. Gao and Q. Liu, *Chem. Commun.*, 2009, 1076.

32 W. Chen, Z. Fan and Z. Lai, *J. Mater. Chem. A*, 2013, **1**, 13862.

33 Z. X. Jiang, L. Geng, Y. D. Huang, S. A. Guan, W. Dong and Z. Y. Ma, *J. Colloid Interface Sci.*, 2010, **354**, 866.

34 Y. C. Sang, A. B. Albadarin, A. H. Al-Muhtaseb, C. Mangwandi, J. N. McCracken, S. E. J. Beli and G. M. Walker, *Appl. Surf. Sci.*, 2015, **335**, 107.

35 J. Li, L. Yan, H. Li, W. Li, F. Zha and Z. Lei, *J. Mater. Chem. A*, 2015, **3**, 14696.

36 M. Hara, T. Kondon, M. Komoda, S. Ikeda, J. N. Kondo, K. Domen, M. Hara, K. Shinohara and A. Tanaka, *Chem. Commun.*, 1998, 357.

37 G. Kwak, M. Seol, Y. Tak and K. Yong, *J. Phys. Chem. C*, 2009, **113**, 12085.

38 P. Sawunyama, L. Jiang, A. Fujishima and K. Hashimoto, *J. Phys. Chem. B*, 1997, **101**, 11000.

39 F. Kimura, J. Umemura and T. Takenaka, *Langmiur*, 1986, **2**, 96.